ACS Infectious Diseases

pubs.acs.org/journal/aidcbc

Article

Plasmodium falciparum Eukaryotic Translation Initiation Factor 3 is Stabilized by Quinazoline-Quinoline Bisubstrate Inhibitors

Irina Dobrescu, Elie Hammam, Jerzy M. Dziekan, Aurélie Claës, Ludovic Halby, Peter Preiser, Zbynek Bozdech, Paola B. Arimondo, Artur Scherf,* and Flore Nardella*

Cite This: *ACS Infect. Dis.* 2023, 9, 1257–1266

Read Online

ACCESS | Metrics & More | Article Recommendations | Supporting Information

ABSTRACT: Malaria drug resistance is hampering the fight against the deadliest parasitic disease affecting over 200 million people worldwide. We recently developed quinoline-quinazoline-based inhibitors (as compound **70**) as promising new antimalarials. Here, we aimed to investigate their mode of action by using thermal proteome profiling (TPP). The eukaryotic translation initiation factor 3 (EIF3i) subunit I was identified as the main target protein stabilized by compound **70** in *Plasmodium falciparum*. This protein has never been characterized in malaria parasites. *P. falciparum* parasite lines were generated expressing either a HA tag or an inducible knockdown of the PfEIF3i gene to further characterize the target protein. PfEIF3i was stabilized in the presence of compound **70** in a cellular thermal shift Western blot assay, pointing that PfEIF3i indeed interacts with quinoline-quinazoline-based inhibitors. In addition, PfEIF3i-inducible knockdown blocks intra-erythrocytic development in the trophozoite stage, indicating that it has a vital function. We show that PfEIF3i is mostly expressed in late intra-erythrocytic stages and localizes in the cytoplasm. Previous mass spectrometry reports show that PfEIF3i is expressed in all parasite life cycle stages. Further studies will explore the potential of PfEIF3i as a target for the design of new antimalarial drugs active all along the life cycle of the parasite.

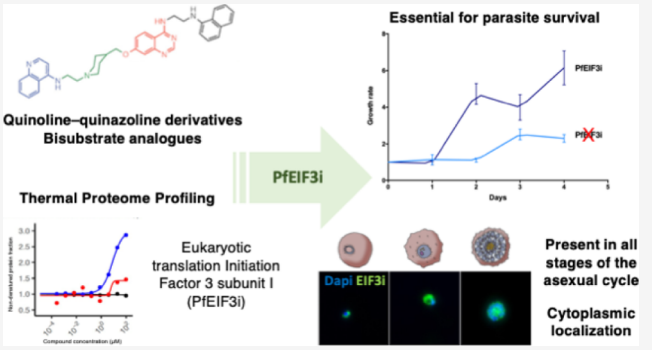

KEYWORDS: *malaria, bisubstrate inhibitors, TPP assay, eukaryotic translation initiation factor 3 subunit I, antimalarial target*

Plasmodium falciparum is the malaria parasite responsible for the majority of the 619,000 deaths and the 247 million cases worldwide reported in 2021.[1] *P. falciparum* infection can cause severe clinical symptoms such as anemia, respiratory distress, and, in the most complicated cases, cerebral malaria. Parasite multi-drug resistance to the main line therapy, consisting of artemisinin-based combination therapies, has emerged in South-East Asia causing first-line treatment failures.[2] Our group recently developed quinoline-quinazoline-based inhibitors designed to inhibit DNA methyltransferases (DNMT) by binding the two substrate pockets of these enzymes (thus named "bisubstrate" inhibitors). The quinazoline moiety mimics the adenosine group of the methyl donor, the *S*-adenosyl-L-methionine (SAM), and the quinoline moiety mimics the cytidine, the methylation substrate[3] (Figure 1A). Repurposing these compounds for malaria therapy enabled us to identify compound **70** as the most potent compound of the chemical series, with an IC_{50} of 60 nM against *P. falciparum*. This compound is a fast-acting antimalarial, active in the ring-stage survival assay against artemisinin-resistant field isolates, with a promising in vivo activity in a mouse malaria model.[4] We have shown that it reduces the activity of DNA methyltransferases (DNMT) to methylate DNA cytosines in human cells as well as in *P. falciparum* protein extracts. However, the only annotated DNMT in *Plasmodium*, DNMT2, is in fact mostly methylating *t*-RNA and is dispensable in asexual blood stages,[5] making DNA cytosine methylation not likely to be the primary drug target. Thus, the target protein of this family of compounds remains to be identified.

In this study, we explored the mode of action in malaria parasites of this family of quinoline-quinazoline inhibitors by using the thermal proteome profiling (TPP),[6−8] in which the proteome in the presence and absence of the compound is analyzed by mass spectrometry at different temperatures. The assay is based on the principle that the stability of a protein changes upon interactions with a ligand, such as inhibitors.[9] TPP employs pulse thermal challenge to denature unstable protein subsets and quantifies the remaining soluble protein abundance to identify the proteins that are thermally stabilized

Received: March 16, 2023
Published: May 22, 2023

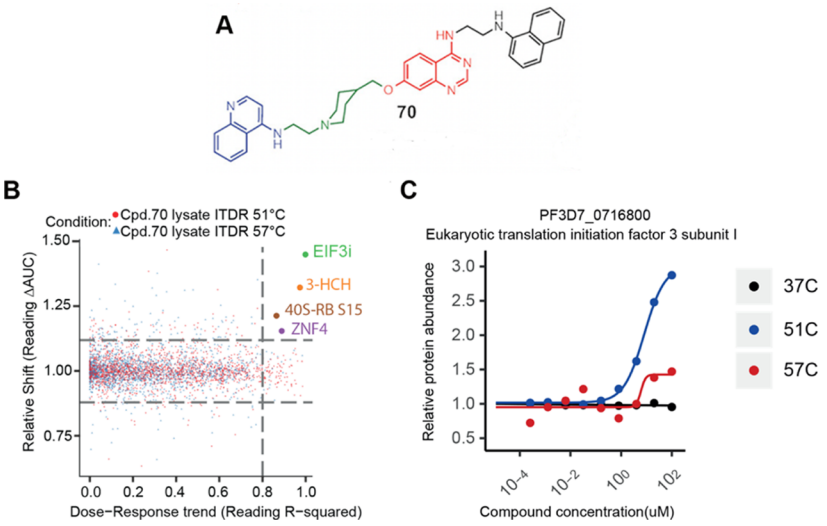

Figure 1. PfEIF3i is stabilized by compound 70. (A) Structure of compound **70**, a DNMT bisubstrate inhibitor repurposed for malaria therapy. The quinazoline moiety (in red) mimics SAM, and the quinoline moiety (in blue) mimics cytidine, separated by a linker (in green). (B) TPP target engagement by compound **70**, obtained in a single experiment. Whole proteome analysis in lysate ITDR (isothermal dose response) experiments under 0−100 μM of compound **70** treatment of parasite extracts during 3 min followed by thermal challenges at 51 °C (blue triangles) or 57 °C (red circles). Distribution of protein stabilization is plotted as a function of R^2 value (goodness of curve fit) against ΔAUC (area under the curve of heat-challenged sample normalized against nondenaturing 37 °C control) for all proteins detected in the assay. Three times of median absolute deviation (MAD) of ΔAUC in each dataset (MAD × 3) and R^2 = 0.8 cutoffs are indicated on the graph. Significant hits are highlighted in other colors: EIF3i (green, PF3D7_0716800) = eukaryotic initiation factor 3 subunit I; 3-HCH (orange, PF3D7_1240000) = 3-hydroxyisobutyryl-CoA hydrolase; 40S-RB S15 (brown, PF3D7_1358800) = 40S ribosomal protein S15; and ZNF4 (violet, PF3D7_1134600) = CCCH-type zinc finger protein ZNF4. TPP stabilization curves of these hits are represented in Table S2. (C) Thermal stabilization profile of EIF3i identified in panel (B). Stabilization under thermal challenges [51 °C (blue) or 57 °C (red)] is plotted relative to no-drug control with non-denaturing control (37 °C) in black.

by the drug. Using this technique, we found the eukaryotic translation initiation factor 3 subunit I (PfEIF3i) as the main protein stabilized by the lead bisubstrate inhibitor **70**.[4]

Eukaryotic translation initiation factors mediate the assembly of tRNA, 40S, and 60S ribosomal subunits into an 80S ribosome at the initiation codon of mRNA, a complex process required for protein synthesis initiation.[10] Among these factors, the largest complex EIF3, containing 13 subunits,[11] has a crucial role in different steps of translation initiation and is involved in termination and ribosomal recycling. Due to its multicomplex network, EIF3 is a major actor in many biological processes and can be associated with functional disorders.[12,13] Its dysregulation is linked to different types of cancers (reviewed in ref 14), suggesting an important role in cell proliferation regulation[15] and in cell cycle differentiation. EIF3i has not been studied in *Plasmodium*, we, therefore, explored the essential functions of this protein in *P. falciparum* blood-stage development.

RESULTS

Identification of Compound 70 Putative Targets by TPP. To identify the candidate target(s) of the bisubstrate inhibitor **70**[4] in *P. falciparum*, parasite protein extracts were treated with increasing concentrations of the compound for 3 min and fractions were then exposed, in parallel, to different temperatures: 37 (non-denaturing control), 51, and 57 °C. The soluble protein abundance in the presence of varying drug concentrations was quantified by mass spectrometry, relative to the vehicle control sample. In total, 1904 individual proteins meet the criteria of a peptide spectrum match (PSM) ≥3 and were detected in the 37 °C control condition, which led to the analysis of 3535 protein stability profile curves, under the 51 and 57 °C thermal challenges. Four proteins were found to exhibit significant (≥3 × median absolute deviation in the Δ Area Under the Curve) drug-concentration-dependent stabilization (Figure 1B, Table S2), including the eukaryotic translation initiation factor 3 subunit I (EIF3i), 40S Ribosomal Protein S15, Zinc Finger Protein, and 3-hydroxyisobutyryl-CoA hydrolase. Among those, EIF3i exhibited the strongest stabilization, achieving nearly three-fold stabilization at the highest drug concentration tested (100 μM) under the 51 °C thermal challenge condition. In this same condition, a concentration of 1.5 μM was sufficient to induce a stabilizing response (Figure 1C). The presumed target of compound **70**, PfDNMT2, was not detected among the 1904 proteins identified in the assay. The full dataset of protein stabilization curves is available in the PDF supplementary file entitled "dataset of protein stability curves".

Compound 70 Stabilizes PfEIF3i. To validate the results obtained in the TPP analysis, a transgenic *P. falciparum* NF54 parasite line was generated by introducing a 3× hemagglutinin epitope tag (3xHA) expressed in frame with *eif3i* (Figure 2A). After verification of the correct genomic integration and HA-tagging of EIF3i (Figure 2B), we used this transgenic parasite strain in the Cellular Thermal Shift Assay (CETSA)[7] analysis followed by Western blot (CETSA-WB). In this assay, parasite protein extracts were treated for 1 h with 30 μM of compound **70** and exposed to different temperatures and analyzed by Western blot to assess the level of the tagged EIF3i protein. Upon increase of the temperature, EIF3i protein is stabilized when treated with compound **70** compared to the DMSO control (Figure 2C). The protein stabilization occurs from 40 °C until 52 °C (Figures 2D, S2), in agreement with the TPP assay, in which pronounced EIF3i stabilization is observed at

https://doi.org/10.1021/acsinfecdis.3c00127
ACS Infect. Dis. 2023, 9, 1257−1266

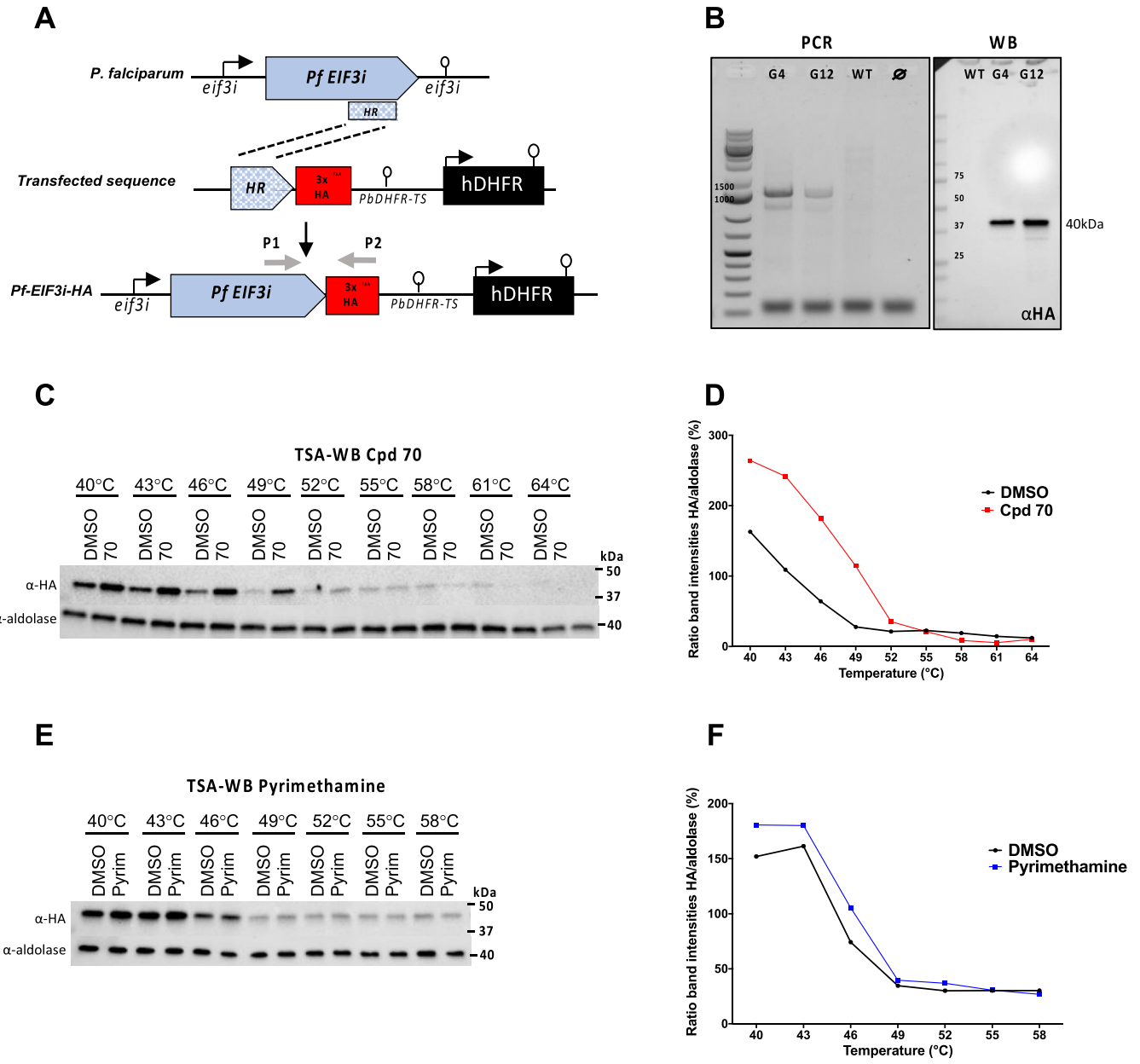

Figure 2. Western blot detection of PfEIF3i stabilization in parasite extracts treated with compound 70. (A) Strategy to generate the PfEIF3i-HA parasite line by tagging EIF3i with the 3xHA tag at the end of the coding sequence (cds). HR: homology region; arrow boxes: coding sequences; arrows: 5′UTR; open circle lollipop: 3′UTR; black box: hDHFR, selection marker cassette; red box: 3xHA-tag; gray arrows P1 and P2, primers used for the PCR. PbDHFR-TS (PBANKA_0719300) regulatory region acts as the 3′-UTR for the HA-recombinant PfEIF3i *locus*. (B) After transfection, the integration was validated by PCR and HA expression was confirmed by Western blot using anti-HA antibodies, in two clones, G4 and G12. (C,D) PfEIF3i-HA extracts were collected, treated with 30 μM of compound **70** for 1 h at RT and exposed to a temperature gradient (40−67 °C). Soluble protein levels were run in an SDS-PAGE gel, and EIF3i levels were quantified by Western blot using anti-HA antibodies; anti-aldolase antibodies were used as loading controls. Band intensities were measured with image lab software (Biorad), and graphs represent the HA signal normalized to the aldolase band intensities in percentage. Results were obtained in two independent experiments; figures are representative of one experiment (see Figure S2 for the second experimental dataset). (E,F) Pyrimethamine was used as a negative control in the same conditions as for compound **70**.

51 °C (Figure 1B). In addition, we observe no protein stabilization when PfEIF3i-HA parasites are treated with pyrimethamine (negative control) at any of the used temperatures (Figure 2E,F).

Inducible PfEIF3i Knockdown. As we confirmed that PfEIF3i interacts with compound **70**, a fast-acting antimalarial agent active in resistant strains, we studied the function of PfEIF3i. To this aim, we generated a second transgenic parasite PfEIF3i-HARibo line that possessed an HA-tag in frame with *eif3i* and an additional *glmS* ribozyme sequence (Figure 3A) allowing the conditional knockdown of the protein upon glucosamine addition.[16] After transfection, selection, and cloning, integration of the sequences was confirmed by PCR using specific primers (Figure 3B). The two positive clones that we selected show correct HA expression in Western blot at a size corresponding to EIF3i protein (37 kDa, Figure 3B). PfEIF3i-HARibo parasites were cultured in the presence or absence of glucosamine over one asexual development cycle

https://doi.org/10.1021/acsinfecdis.3c00127
ACS Infect. Dis. 2023, 9, 1257−1266

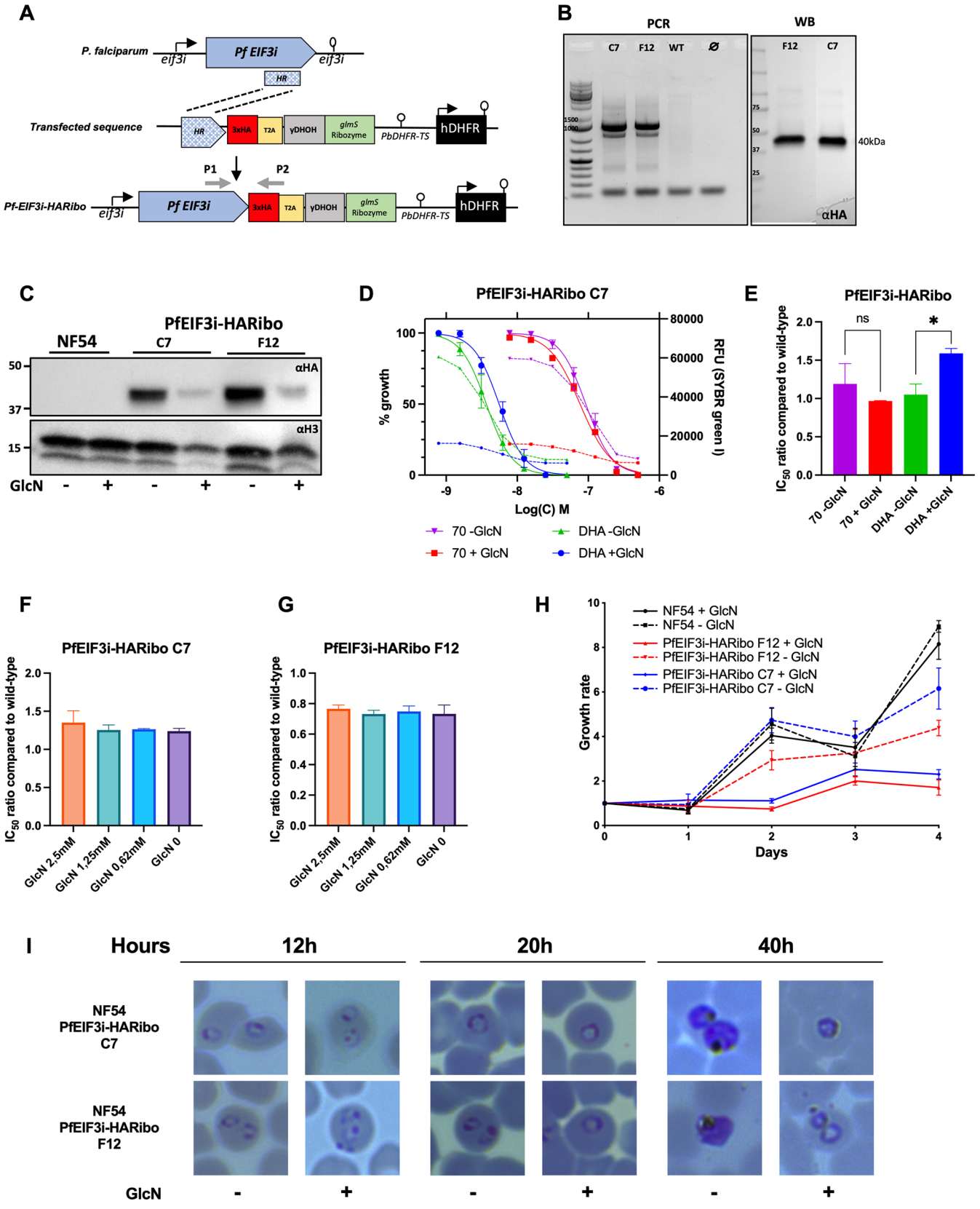

Figure 3. Addition of glucosamine efficiently knocks down PfEIF3i protein levels and impacts growth. (A) Strategy to generate the PfEIF3i-HARibo parasite line with 3xHA tag followed by a *glmS* ribozyme sequence. HR: homology region; arrow boxes: coding sequences; arrow: 5′UTR; open circle lollipop: 3′UTR; black box: hDHFR, selection marker cassette; red box: 3xHA-tag; green box: *glmS* ribozyme cassette; yellow box: T2A peptide; gray box: yDHOH cassette; and gray arrows P1 and P2: primers used for the PCR. PbDHFR-TS (PBANKA_0719300) regulatory region is acting as the 3′-UTR for the HA-recombinant EIF3i *locus*. (B) After transfection, the integration was validated by PCR, and correct HA expression was confirmed by Western blot using anti-HA antibodies. (C) Protein extracts of PfEIF3i-HARibo clones C7 and F12 were collected

https://doi.org/10.1021/acsinfecdis.3c00127
ACS Infect. Dis. 2023, 9, 1257−1266

Figure 3. continued

after saponin lysis from parasite cultured with or without glucosamine (GlcN) for one cycle (48 h). EIF3i protein levels were quantified by Western blot using anti-HA monoclonal antibodies and anti-H3 antibodies as loading controls. (D) IC_{50} curves representing the data obtained for the EIF3i knockdown clone C7 +/− glucosamine (GlcN) treatment for 48 h followed by IC_{50} determination using the SYBR-green I method. The dotted lines represent the raw RFU data obtained in the SYBR green I assay (right axis) that show a near 80% reduction in growth in the GlcN-treated conditions. (E) IC_{50} ratio obtained for compound **70** and DHA, under the conditions described for panel (D) in the PfEIF3i knockdown compared to the wild-type NF54 strain. Histograms represent the mean of two replicates in the two clones, and error bars represent standard deviation. Statistics: student *t*-test to compare the condition plus or minus glucosamine (p_{70} = 0.3573; p_{DHA} = 0.0378). (F,G) IC_{50} ratio obtained for compound **70**, treated with different glucosamine concentrations, in the two PfEIF3i knockdown clones C7 and F12 compared to the wild-type NF54 strain. In this case, glucosamine was added just before parasite plating for IC_{50} determination. (H) Growth curve of the PfEIF3i-HARibo line. Parasites were cultivated in the presence or absence of 2.5 mM GlcN (added at day 0, D0), and growth was assessed for 4 days, every 24 h, by flow cytometry using SYBR green I staining. This experiment was performed once in triplicates. The error bars represent the standard deviation between triplicate values. (I) Synchronized parasites were cultivated in the presence or absence of GlcN (added at t = 0 h), and blood smears were realized regularly at ring, trophozoite, and schizont stages.

(48 h) in order to induce EIF3i protein knockdown. EIF3i protein levels were quantified by Western blot. The two transgenic parasite clones show up to 80% reduction in EIF3i expression after 48 h glucosamine treatment, indicating a successful knockdown of the target protein (Figure 3C).

Knocking Down PfEIF3i Does Not Affect the Sensitivity to Compound 70. To assess the effect of low levels of PfEIF3i on the activity of compound **70**, growth inhibition curves were carried out in two different conditions. Since the effect of glucosamine is only observed after treating the parasites for one cycle, parasites were synchronized and treated over one 48 h cycle with or without glucosamine, and then the effect of compound **70** and dihydroartemisinin (DHA) was assessed by a SYBR-green I assay after 72 h incubation. IC_{50} curves after normalization were plotted (Figure 3D), and they showed no shift in IC_{50} (Figure 3E). However, the growth of the parasites treated with glucosamine was impacted, as revealed by the low RFU values obtained in the SYBR green assay (dotted lines in Figure 3D), which induced a poor *Z*-factor in this condition (Z = 0.81 and 0.84 for the two knocked down clones versus Z = 0.92 for the wild-type line treated with 2.5 mM of glucosamine for one cycle). In the second experiment, we added glucosamine at different concentrations (2.5 to 0.625 mM) just before plating the parasites for the IC_{50} curves. Here, again, no difference in IC_{50} was observed in comparison with the WT line (Figure 3F,G). Since compound **70** is active in less than 6 h, it is possible that the compound is active before EIF3i is depleted. In these experimental conditions, knocking down PfEIF3i did not confirm that this protein is the main target of compound **70**. Overexpression of PfEIF3i using an episome, despite multiple attempts, failed to select for transfected parasites; this could indicate that overexpressing this protein may be deleterious for *Plasmodium*.

PfEIF3i is Essential for Parasite Growth and Localizes to Cytoplasm. Since PfEIF3i has never been described before, we characterized the biological impact of EIF3i on parasite erythrocytic development. *P. falciparum* NF54 and PfEIF3i-HARibo lines were synchronized to obtain ring stage parasites and the parasitemia was followed for two cycles by flow cytometry, with or without glucosamine addition. EIF3i knockdown (EIF3i-KD) parasites (+glucosamine) grow at a slower rate than NF54 and EIF3i-KD parasites cultured without glucosamine (Figure 3H). The growth defect is also observed in Giemsa-stained thin blood smears: PfEIF3i-HARibo parasites at 40 h post-invasion, cultivated with glucosamine, show a delay in maturation (Figure 3I). Therefore, EIF3i seems to be essential for parasite intra-erythrocytic development. The protein is expressed in all intra-erythrocytic stages but mostly in trophozoites and schizonts (Figure 4A); interestingly, these are the stages that are more sensitive to compound **70**.[4] EIF3i localization in *P. falciparum* parasite was assessed by immunofluorescence (IFA), using anti-HA antibodies (Figure 4B). The IFA shows a cytoplasmic localization of the EIF3i protein in ring, trophozoites, and schizonts, in agreement with its localization in human cells.[12,14]

DISCUSSION

To decipher the mode of action of the quinoline-quinazoline-based inhibitors that we previously identified as potent new antimalarials,[4] we applied the TPP[9,17,18] technique and identified binding-partners and potential targets of the bisubstrate compound **70** in asexual blood stages of *P. falciparum*. PfDNMT2 was not detected among the 1904 proteins identified, so its thermo-stabilization in the presence of compound **70** is unknown. However, this protein is not likely to be the target responsible for the anti-proliferative effect since we demonstrated that knocking out PfDNMT2 allows the parasites to grow normally.[5] Also, when we tested compound **70** in the DNMT2 KO line, we found no difference in IC_{50} compared to the wild-type (22.9 nM in the WT 3D7A versus 20.5 and 25.3 nM in the two PfDNMT2 KO clones; Figure S1). Among the proteins stabilized by the inhibitor in TPP, we explored PfEIF3i, which showed the best stabilization curve (Figure 1, Table S2). We engineered a transgenic *P. falciparum* line expressing PfEIF3i tagged with 3xHA to confirm that PfEIF3i is stabilized by compound **70** by CETSA-WB. We also engineered an inducible knockdown of PfEIF3i. However, this line did not confirm PfEIF3i as the primary target of compound **70**. This might be explained by different reasons: compound **70** could have polypharmacology and thus additional targets that contribute to the effect; knocking down PfEIF3i could have a broader effect, like destabilizing the complex or down-regulating other subunits of the complex, similar to what has been observed in human cells;[11] finally, the inability to obtain a line overexpressing EIF3i could indicate the fine regulation of this protein complex and a sophisticated inhibition mechanism that does not necessarily rule out PfEIF3i as the primary target. Indeed, by studying bacterial drug-resistance mechanisms, Palmer and Kishony showed that depending on the molecular mechanism of the inhibitor, overexpressing (and alternatively knocking-down) a protein target is not always associated with an IC_{50} shift.[19] As PfEIF3i has never been characterized in *Plasmodium*, we further studied its function in the parasite. The inducible

https://doi.org/10.1021/acsinfecdis.3c00127
ACS Infect. Dis. 2023, 9, 1257−1266

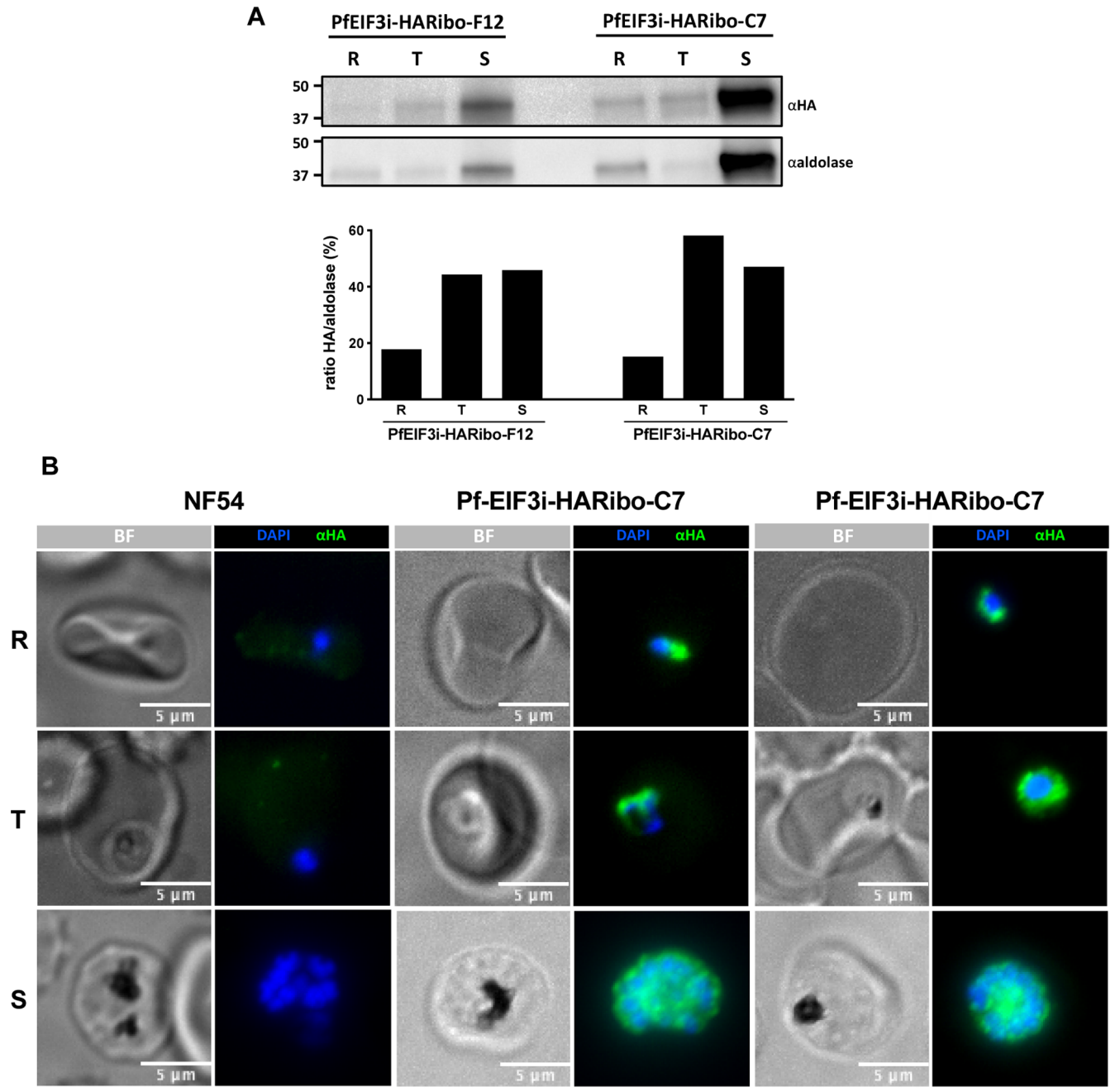

Figure 4. PfEIF3i is expressed in all intra-erythrocytic stages and localizes to the cytoplasm. (A) Protein extracts of PfEIF3i-HARibo clones C7 and F12 were collected after saponin lysis from ring (R), trophozoite (T), and schizont (S) stages. EIF3i protein levels were quantified by Western blot using anti-HA monoclonal antibodies and anti-aldolase antibodies as loading controls. Graph represents the ratio of HA/aldolase band intensities expressed in percentage. (B) Immunofluorescence assays of fixed RBCs infected with *Plasmodium falciparum* NF54 or PfEIF3i-HARibo parasites clones C7 and F12 at ring (R), trophozoite (T), and schizont (S) stages. EIF3i-HA was detected using anti-HA antibodies (green), and DNA was stained with DAPI (blue).

knockdown of PfEIF3i allowed us to characterize for the first time a subunit of the PfEIF3 complex. As predicted,[20] the protein is essential for the survival of the parasite as it blocks parasite development at the trophozoite stage when the protein is knocked down by approximately 80%. PfEIF3i is expressed in the different stages of *P. falciparum* asexual blood cycle, which is in accordance with the asexual blood stage (ABS) activity that we described for compound **70**:[4] this compound is active against all stages of the ABS, but trophozoites and schizonts between 12 and 36 h post-invasion are the most sensitive. Also, based on the mass spectrometry datasets available in the *Plasmodium* database (PlasmoDB, plasmodb.org), PfEIF3i is expressed in all life cycle stages of *P. falciparum*: asexual stages,[21] gametocytes,[22] and mosquito stages[23] (ookinetes, oocyst, and sporozoite). This protein is well conserved in eukaryotes, and the EIF3 complex plays a key role in translation initiation and termination.[24]

In mammals, this large complex (approximately 800 kDa) is composed of 13 subunits, EIF3a-m.[25] Assembled together, the subunits participate in several steps of translation initiation, termination ribosomal recycling, and stimulation of stop codon readthrough.[26−29] In PlasmoDB, only 12 EIF3 subunits are

https://doi.org/10.1021/acsinfecdis.3c00127
ACS Infect. Dis. 2023, 9, 1257−1266

annotated, but none have been studied yet. Among the PfEIF3 complex, only PfEIF3i is stabilized by compound **70**, the other subunits were found in the analysis but were not stabilized (Table S3). The PfEIF3 complex might have a role in drug resistance:[11] in mefloquine-resistant *P. falciparum* strains, PfEIF3 was shown to be upregulated in a protein profiling analysis by mass spectrometry.[30] *Leishmania infantum* resistance to amphotericin-B was also associated with higher expression levels of EIF3.[31] PfEIF3i was also found in a mass spectrometry-coupled cellular TSA (MS-CETSA) as a potential hit target of chloroquine, even though it was not identified in the labeled activity-based protein profiling (ABPP) used in parallel.[32] As bisubstrate inhibitors share a quinoline moiety in their scaffold with chloroquine, finding a common stabilized protein is not surprising.

In conclusion, it is important to identify the targets of compounds that are potent antimalarials to use them in combination to anticipate as well as to monitor resistance during further deployment.[33] Here, we report PfEIF3i, directly interacting with the quinazoline-quinoline bisubstrate inhibitor **70**. PfEIF3i is essential for the parasite development and is expressed throughout the intraerythrocytic stages of *P. falciparum* and is detected by mass spectrometry in the different stages of the malaria life cycle. Further work will focus on characterizing PfEIF3i potential as a drug target.

METHODS

Thermal Proteome Profiling. Experiments were carried out as previously described[17] with minor modifications. Briefly, *P. falciparum* trophozoite lysate was exposed to varying concentrations of compound **70** (100 μM-0.25 nM) and a DMSO control for 3 min, followed by thermal challenge at 37, 51, or 57 °C. Remaining soluble protein was analyzed by quantitative mass spectrometry. In each experimental set, TMT10-plex-labeled peptides were pulled together, fractionated via high-pH reversed phase chromatography, and analyzed by LC−MS/MS (ThermoFisher Scientific Q-Exactive HF) with 40 1 ug peptide injections on a pre-programmed 70 min gradient of solvent A (0.1% formic acid in water) and solvent B (0.1% formic acid in acetonitrile). MS/MS data analysis was carried out in Proteome Discoverer 2.1, using precursor mass error of 20 ppm, fragment mass error of 0.05 Da, Carbamidomethylation (C) and TMT6plex (K, N-term) as static modifications and Oxidation (M), Deamidation (NQ), and Acetylation (Protein N-term) as dynamic modifications. Downstream data processing was carried out in the R environment, using mineCETSA package 1.1.1. Proteins exhibiting drug dose-dependent change in stability were identified using a set of criteria, including ≥3PSM, $R^2 \geq 0.8$, $\Delta AUC \geq 3 \times MAD$. The experiment was performed once.

Plasmid Constructs. The pSLI-HA-FKBP-T2A-yDHOH-Ribozyme plasmid was generated in our laboratory from the pSLI plasmid[34] by In-fusion (Takara) insertion of five PCR fragments coding for 3× hemagglutinin epitope tag (3xHA), FKBP, T2A peptide, yeast dihydroorotate dehydrogenase (yDHODH), and *glmS* ribozyme sequences. The pSLI-EIF3i-HA plasmid was generated from the pSLI-HA-FKBP-T2A-yDHOH-Ribozyme plasmid by In-fusion of two PCR fragments coding for the last 845 bp of *eif3i* cds (PlasmoDB:[35] PF3D7_0716800, primers P3F−P3R) and 3xHA (primers P4F−P4R) at NotI/XhoI restriction sites to replace FKBP, T2A, yDHODH, and *glmS* ribozyme sequences. The pSLI-EIF3i-HARibo plasmid was generated from the pSLI-HA-FKBP-T2A-yDHOH-Ribozyme plasmid by In-fusion of two PCR fragments coding for the last 845 bp of *eif3i* cds (primers P3F−P3R) and 3xHA (primers P5F−P5R) at NotI/SalI restriction sites to remove the FKBP sequence. All PCR were performed using KAPA HiFi DNA Polymerase (Roche 0795884600) with primers described in Supporting Information Table 1. The last 845 bp of *eif3i* were PCR-amplified from genomic *P. falciparum* NF54 DNA. The stop codon was removed from the original sequence and added after the 3xHA tag so it can be expressed with the *eif3i* gene. The final constructs are depicted in Figures 2A and 3A, and primers used in this study are described in the Supporting Information (Table S1).

Parasite Culture and Transfection. *P. falciparum* parasites were cultured using a standard protocol.[36] The laboratory strain used was NF54. Parasite transfections were done by electroporation of ring stages using 50 μg of purified plasmid NucleoBond Xtra kit (Macherey Nagel), as described elsewhere.[37,38] Drug selection was done using 2.66 nM of WR99210 (Jacobus Pharmaceuticals) for 5 days after transfection. After homologous recombination parasites were cloned by serial dilution,[39] PfEIF3i knockdown was achieved upon addition of 2.5 mM of glucosamine for 48 h (Sigma, G1415).

Growth Inhibition Assay Using PfEIF3i Knockdown Line. To assess the effect of low levels of PfEIF3i on the activity of compound **70**, growth inhibition curves were carried out in two different conditions, in the PfEIF3i-HARibo line and in the NF54 wild-type strain: since the effect of glucosamine is only seen after treating the parasites for one cycle, we synchronized parasites, treated them over one cycle (48 h) with or without glucosamine, and then assessed the effect of compound **70** and dihydroartemisinin (DHA), starting at ring-stage, using 72 h incubation followed by a SYBR-green I assay, following the protocol that we described in ref 4 (7-point 2-step dilutions starting at 500 nM for compound **70** and 50 nM for DHA; 2% hematocrit, 0.7% starting parasitemia using mostly ring stage culture). In a second experiment, we added glucosamine at different concentrations (2.5, 1.25, 0.625, and 0 mM) just before plating the parasites for the IC_{50} curves and incubated parasites for 72 h followed by a SYBR-green I assay, following the protocol described in ref 4.

Western Blot. Parasites were harvested using 0.15% saponin lysis of infected RBC (iRBC), followed by PBS washes. Proteins of the parasite pellets were extracted using lysis buffer (1 mM DTT, 2× Laemmli buffer (Bio-Rad, 161−0737), and protease inhibitor cocktail (Roche, 11836170001) dissolved in PBS and sonicated for 5 min (30sec on/off cycles). The equivalent of 1×10^7 parasites was loaded per lane in a 4−20% Mini-PROTEAN TGX Stain-Free gel (Bio-Rad, 4568096), and proteins were separated and transferred onto a nitrocellulose membrane using the transblot semi-wet transfer system (Bio-Rad). Blocking and antibody dilutions were performed in PBS-Tween-20 with 5% skim milk. Anti-HA (Abcam, ab9110), HRP-anti-*Plasmodium* aldolase (Abcam, ab38905), and anti-H3 (Abcam, ab1791) were used at 1:1000; secondary anti-rabbit HRP antibody was diluted at 1:5000. The blot was revealed using a Super Signal West-Femto chemiluminescent substrate (Thermo Fisher Scientific).

CETSA-Western Blot. Approximately 3×10^8 parasites were harvested through saponin lysis, snap-frozen, and stored at −80 °C until further use. Parasite lysates were realized by

https://doi.org/10.1021/acsinfecdis.3c00127
ACS Infect. Dis. 2023, 9, 1257−1266

diluting the parasite pellet in 1 ml of PBS, followed by lysis using repetitive freeze/thaw cycles (−80 °C to room temperature—RT). The parasite lysates were then treated with 30 μM of compound **70**[4] or 30 μM of pyrimethamine or the equivalent volume of DMSO for 1 h at RT. Then the treated lysates were divided into 10 tubes of 100 μl and exposed to a 10-point temperature challenge, from 40 to 67 °C (3 °C-fold increment), for 5 min. After 3 min at RT, tubes were centrifuged at 15,000*g* for 20 min at 4 °C. Soluble proteins contained in the supernatant were separated and mixed with 4× Laemmli sample buffer (Bio-Rad, 161−0747) before being loaded on an SDS-PAGE gel (4−20% Criterion TGX Stain-Free Protein Gel, Bio-Rad #5678095). Western blot was then performed as described in the previous section. The experiment was performed in two independent experiments.

Growth Curve. Parasites were synchronized at the ring stage and incubated with fresh red blood cells at a starting parasitemia of 0.2%. Each day 20 μl of the culture was collected and fixed with 0.025% glutaraldehyde and quenched after 1 h with 15 mM of ammonium chloride (NH_4Cl). Fixed cells were then stained with 2X SYBR Green I (Lonza, 50512), and parasitemia was determined by flow cytometry using the Guava EasyCyte HT flow cytometer (Luminex).

Immunofluorescence. iRBCs were fixed with 4% paraformaldehyde (EMS 15714) and 0.0075% glutaraldehyde (EMS 16220) in PBS for 30 min, as described previously (Tonkin et al., 2004). After PBS wash, cells were permeabilized with 0.1% Triton-X100 for 10 min, and free aldehyde groups were quenched with 50 mM NH_4Cl for 10 min. Then cells were blocked with 1% bovine serum albumin (BSA) (Sigma A4503-50G) in PBS for 30 min and incubated overnight at 4 °C with 1:1500 anti-HA high affinity (Roche, 3F10). After three PBS washes, goat anti-rat Alexa Fluor 488 (Invitrogen, A-11006) secondary antibody was used at 1:2000 with DAPI (FluoProbes FP-CJF800, 1 μg/mL). Finally, cells were mounted with VectaShield (Vector Laboratories, H-1000) on glass slide. Images were acquired on a Deltavision Elite imaging system (Leica) and processed using ImageJ-FiJi software.[40]

■ ASSOCIATED CONTENT

Supporting Information

The Supporting Information is available free of charge at https://pubs.acs.org/doi/10.1021/acsinfecdis.3c00127.

Table S1 references the PCR primers used in this study, Table S2 references TPP stabilization curves of hits reported in Figure 1B, and Table S3 represents the thermal stabilization curves of the 12 annotated proteins found in the PfEIF3i complex. Figure S1 represents the IC_{50} curves obtained for compound **70** in the PfDNMT2-KO parasites, Figure S2 represents the 2nd independent experiment of the Western blot detection of PfEIF3i stabilization in parasite extracts treated with compound **70**. Additional supplementary file "dataset of protein stability curves" represents the TPP stabilization curves obtained for all the proteins identified in the study (PDF)

(PDF)

■ AUTHOR INFORMATION

Corresponding Authors

Artur Scherf − *Unité Biology of Host-Parasite Interactions, Department of Parasites and Insect Vectors, Institut Pasteur, Université de Paris-Cité, CNRS EMR 9195, INSERM Unit U1201, Paris 75015, France*; Email: artur.scherf@pasteur.fr

Flore Nardella − *Unité Biology of Host-Parasite Interactions, Department of Parasites and Insect Vectors, Institut Pasteur, Université de Paris-Cité, CNRS EMR 9195, INSERM Unit U1201, Paris 75015, France*; orcid.org/0000-0002-3811-1633; Email: flore.nardella@gmail.com

Authors

Irina Dobrescu − *Unité Biology of Host-Parasite Interactions, Department of Parasites and Insect Vectors, Institut Pasteur, Université de Paris-Cité, CNRS EMR 9195, INSERM Unit U1201, Paris 75015, France*

Elie Hammam − *Unité Biology of Host-Parasite Interactions, Department of Parasites and Insect Vectors, Institut Pasteur, Université de Paris-Cité, CNRS EMR 9195, INSERM Unit U1201, Paris 75015, France*

Jerzy M. Dziekan − *School of Biological Sciences, Nanyang Technological University, Singapore 639798, Singapore*

Aurélie Claës − *Unité Biology of Host-Parasite Interactions, Department of Parasites and Insect Vectors, Institut Pasteur, Université de Paris-Cité, CNRS EMR 9195, INSERM Unit U1201, Paris 75015, France*

Ludovic Halby − *Epigenetic Chemical Biology, Department of Structural Biology and Chemistry, Institut Pasteur, Université de Paris-Cité, UMR n3523 Chem4Life, CNRS, Paris 75015, France*

Peter Preiser − *School of Biological Sciences, Nanyang Technological University, Singapore 639798, Singapore*

Zbynek Bozdech − *School of Biological Sciences, Nanyang Technological University, Singapore 639798, Singapore*

Paola B. Arimondo − *Epigenetic Chemical Biology, Department of Structural Biology and Chemistry, Institut Pasteur, Université de Paris-Cité, UMR n3523 Chem4Life, CNRS, Paris 75015, France*

Complete contact information is available at: https://pubs.acs.org/10.1021/acsinfecdis.3c00127

Author Contributions

The manuscript was written with contribution from all authors. All authors have given approval to the final version of the manuscript.

Notes

The authors declare no competing financial interest.

■ ACKNOWLEDGMENTS

This work was supported by Institut Pasteur-Institut Carnot (S-CR18089-02B15 DARRI CONSO INNOV 46−19; S-PI15006-10A INNOV 05−2019 ARIMONDO IARP 2019 PC), Pasteur Transversal Research Program (PTR 233−2019 HALBY), Pasteur Swiss Foundation grant, Agence Nationale de la Recherche (ANR EpiKillMal), and Pasteur-Roux-Cantarini Fellowship. Zbynek Bozdech's contribution to the work was funded by the Singapore Ministry of Education grant number MOE-T2EP30120-0015, Jerzy Dziekan was funded by a NTU-PPF-2019 grant, and Peter Preiser contribution was supported by the National Research Foundation (Singapore)

grant NRF-CRP24-2020-0005. Elie Hammam's travel to Singapore was funded by the Merlion grant. The authors would like to thank Jessica Bryant of the Host Parasite Interactions unit at the Institut Pasteur for the pSLI-HA-FKBP-T2A-yDHOH-Ribozyme plasmid.

■ ABBREVIATIONS

ABPP, activity-based protein profiling; ACTs, artemisinin-based combination therapies; AUC, area under the curve; cds, coding sequence; CETSA, cellular thermal shift assay; DNMT, DNA methyltransferase; EIF3, eukaryotic translation initiation factor 3; GlcN, glucosamine; HA, hemagglutinin; iRBC, infected red blood cells; ITDR, isothermal dose response; MAD, median absolute deviation; MS-CETSA, mass spectrometry-coupled cellular thermal shift assay; NH4Cl, ammonium chloride; PlasmoDB, Plasmodium database; TPP, thermal proteome profiling; yDHODH, yeast dihydroorotate dehydrogenase

■ REFERENCES

(1) *World Malaria Report 2022*: World Health Organization: Geneva; 2022. Licence: CC BY-NC-SA 3.0 IGO.
(2) Menard, D.; Dondorp, A. Antimalarial Drug Resistance: A Threat to Malaria Elimination. *Cold Spring Harbor Perspect. Med.* **2017**, *7*, a025619.
(3) Halby, L.; Menon, Y.; Rilova, E.; Pechalrieu, D.; Masson, V.; Faux, C.; Bouhlel, M. A.; David-Cordonnier, M. H.; Novosad, N.; Aussagues, Y.; Samson, A.; Lacroix, L.; Ausseil, F.; Fleury, L.; Guianvarc'H, D.; Ferroud, C.; Arimondo, P. B. Rational Design of Bisubstrate-Type Analogues as Inhibitors of DNA Methyltransferases in Cancer Cells. *J. Med. Chem.* **2017**, *60*, 4665−4679.
(4) Nardella, F.; Halby, L.; Hammam, E.; Erdmann, D.; Cadet-Daniel, V.; Peronet, R.; Ménard, D.; Witkowski, B.; Mecheri, S.; Scherf, A.; Arimondo, P. B. DNA Methylation Bisubstrate Inhibitors Are Fast-Acting Drugs Active against Artemisinin-Resistant Plasmodium Falciparum Parasites. *ACS Cent. Sci.* **2020**, *6*, 16−21.
(5) Hammam, E.; Sinha, A.; Baumgarten, S.; Nardella, F.; Liang, J.; Miled, S.; Bonhomme, F.; Erdmann, D.; Arcangioli, B.; Arimondo, P. B.; Dedon, P.; Preiser, P.; Scherf, A. Malaria Parasite Stress Tolerance Is Regulated by DNMT2- Mediated TRNA Cytosine Methylation. *mBio* **2021**, *12*, No. e02558.
(6) Jafari, R.; Almqvist, H.; Axelsson, H.; Ignatushchenko, M.; Lundbäck, T.; Nordlund, P.; Molina, D. M. The Cellular Thermal Shift Assay for Evaluating Drug Target Interactions in Cells. *Nat. Protoc.* **2014**, *9*, 2100−2122.
(7) Molina, D. M.; Jafari, R.; Ignatushchenko, M.; Seki, T.; Larsson, E. A.; Dan, C.; Sreekumar, L.; Cao, Y.; Nordlund, P. Monitoring Drug Target Engagement in Cells and Tissues Using the Cellular Thermal Shift Assay. *Science* **2013**, *341*, 84−87.
(8) Dziekan, J. M.; Yu, H.; Chen, D.; Dai, L.; Wirjanata, G.; Larsson, A.; Prabhu, N.; Sobota, R. M.; Bozdech, Z.; Nordlund, P. Identifying Purine Nucleoside Phosphorylase as the Target of Quinine Using Cellular Thermal Shift Assay. *Sci. Transl. Med.* **2019**, *11*, No. eaau3174.
(9) Mateus, A.; Kurzawa, N.; Becher, I.; Sridharan, S.; Helm, D.; Stein, F.; Typas, A.; Savitski, M. M. Thermal Proteome Profiling for Interrogating Protein Interactions. *Mol. Syst. Biol.* **2020**, *16*, 9232.
(10) Pestova, T. V.; Kolupaeva, V. G.; Lomakin, I. B.; Pilipenko, E. V.; Shatsky, I. N.; Agol, V. I.; Hellen, C. U. T. Molecular Mechanisms of Translation Initiation in Eukaryotes. *Proc. Natl. Acad. Sci. U. S. A.* **2001**, *98*, 7029−7036.
(11) Gomes-Duarte, A.; Lacerda, R.; Menezes, J.; Romão, L. EIF3: A Factor for Human Health and Disease. *RNA Biol.* **2018**, *15*, 26−34.
(12) Zhang, L.; Pan, X.; Hershey, J. W. B. Individual Overexpression of Five Subunits of Human Translation Initiation Factor EIF3 Promotes Malignant Transformation of Immortal Fibroblast Cells. *J. Biol. Chem.* **2007**, *282*, 5790−5800.
(13) Mata, J. Translation Factors Specify Cellular Metabolic State. *Cell Rep.* **2016**, *16*, 1787−1788.
(14) Ma, S.; Dong, Z.; Cui, Q.; Liu, J. Y.; Zhang, J. T. EIF3i Regulation of Protein Synthesis, Cell Proliferation, Cell Cycle Progression, and Tumorigenesis. *Cancer Lett.* **2021**, *500*, 11−20.
(15) Hershey, J. W. B. The Role of EIF3 and Its Individual Subunits in Cancer. *Biochim. Biophys. Acta, Gene Regul. Mech.* **2015**, *1849*, 792−800.
(16) Prommana, P.; Uthaipibull, C.; Wongsombat, C.; Kamchonwongpaisan, S.; Yuthavong, Y.; Knuepfer, E.; Holder, A. A.; Shaw, P. J. Inducible Knockdown of Plasmodium Gene Expression Using the GlmS Ribozyme. *PLoS One* **2013**, *8*, No. e73783.
(17) Dziekan, J. M.; Wirjanata, G.; Dai, L.; Go, K. D.; Yu, H.; Lim, Y. T.; Chen, L.; Wang, L. C.; Puspita, B.; Prabhu, N.; Sobota, R. M.; Nordlund, P.; Bozdech, Z. Cellular Thermal Shift Assay for the Identification of Drug-Target Interactions in the Plasmodium Falciparum Proteome. *Nat. Protoc.* **2020**, *15*, 1881−1921.
(18) Franken, H.; Mathieson, T.; Childs, D.; Sweetman, G. M. A.; Werner, T.; Tögel, I.; Doce, C.; Gade, S.; Bantscheff, M.; Drewes, G.; Reinhard, F. B. M.; Huber, W.; Savitski, M. M. Thermal Proteome Profiling for Unbiased Identification of Direct and Indirect Drug Targets Using Multiplexed Quantitative Mass Spectrometry. *Nat. Protoc.* **2015**, *10*, 1567−1593.
(19) Palmer, A. C.; Kishony, R. Opposing Effects of Target Overexpression Reveal Drug Mechanisms. *Nat. Commun.* **2014**, *5*, 4296.
(20) Zhang, M.; Wang, C.; Otto, T. D.; Oberstaller, J.; Liao, X.; Adapa, S. R.; Udenze, K.; Bronner, I. F.; Casandra, D.; Mayho, M.; Brown, J.; Li, S.; Swanson, J.; Rayner, J. C.; Jiang, R. H. Y.; Adams, J. H. Uncovering the Essential Genes of the Human Malaria Parasite Plasmodium Falciparum by Saturation Mutagenesis. *Science* **2018**, *360*, No. eaap7847.
(21) Oehring, S. C.; Woodcroft, B. J.; Moes, S.; Wetzel, J.; Dietz, O.; Pulfer, A.; Dekiwadia, C.; Maeser, P.; Flueck, C.; Witmer, K.; Brancucci, N. M. B.; Niederwieser, I.; Jenoe, P.; Ralph, S. A.; Voss, T. S. Organellar Proteomics Reveals Hundreds of Novel Nuclear Proteins in the Malaria Parasite Plasmodium Falciparum. *Genome Biol.* **2012**, *13*, R108.
(22) Florens, L.; Washburn, M. P.; Raine, J. D.; Anthony, R. M.; Grainger, M.; Haynes, J. D.; Moch, J. K.; Muster, N.; Sacci, J. B.; Tabb, D. L.; Witney, A. A.; Wolters, D.; Wu, Y.; Gardner, M. J.; Holder, A. A.; Sinden, R. E.; Yates, J. R.; Carucci, D. J. A Proteomic View of the Plasmodium Falciparum Life Cycle. *Nature* **2002**, *419*, 520−526.
(23) Lindner, S. E.; Swearingen, K. E.; Shears, M. J.; Walker, M. P.; Vrana, E. N.; Hart, K. J.; Minns, A. M.; Sinnis, P.; Moritz, R. L.; Kappe, S. H. I. Transcriptomics and Proteomics Reveal Two Waves of Translational Repression during the Maturation of Malaria Parasite Sporozoites. *Nat. Commun.* **2019**, *10*, 4964.
(24) Kaur, C.; Kumar, M.; Patankar, S. Messenger RNAs with Large Numbers of Upstream Open Reading Frames Are Translated via Leaky Scanning and Reinitiation in the Asexual Stages of Plasmodium Falciparum. *Parasitology* **2020**, *147*, 1100−1113.
(25) des Georges, A.; Dhote, V.; Kuhn, L.; Hellen, C. U.; Pestova, T. V.; Frank, J.; Hashem, Y. Structure of Mammalian EIF3 in the Context of the 43S Preinitiation Complex. *Nature* **2015**, *525*, 491−495.
(26) Shivaya Valasek, L. 'Ribozoomin' − Translation Initiation from the Perspective of the Ribosome-Bound Eukaryotic Initiation Factors (EIFs). *Curr. Protein Pept. Sci.* **2012**, *13*, 305−330.
(27) Beznosková, P.; Wagner, S.; Jansen, M. E.; von der Haar, T.; Valášek, L. S. Translation Initiation Factor EIF3 Promotes Programmed Stop Codon Readthrough. *Nucleic Acids Res.* **2015**, *43*, 5099−5111.
(28) Beznosková, P.; Cuchalová, L.; Wagner, S.; Shoemaker, C. J.; Gunišová, S.; von der Haar, T.; Valášek, L. S. Translation Initiation Factors EIF3 and HCR1 Control Translation Termination and Stop Codon Read-through in Yeast Cells. *PLoS Genet.* **2013**, *9*, No. e1003962.

https://doi.org/10.1021/acsinfecdis.3c00127
ACS Infect. Dis. 2023, 9, 1257−1266

(29) Pisarev, A. V.; Hellen, C. U. T.; Pestova, T. V. Recycling of Eukaryotic Post-Termination Ribosomal Complexes. *Cell* **2007**, *131*, 286−299.
(30) Reamtong, O.; Srimuang, K.; Saralamba, N.; Sangvanich, P.; Day, N. P. J.; White, N. J.; Imwong, M. Protein Profiling of Mefloquine Resistant Plasmodium Falciparum Using Mass Spectrometry-Based Proteomics. *Int. J. Mass Spectrom.* **2015**, *391*, 82−92.
(31) Brotherton, M. C.; Bourassa, S.; Légaré, D.; Poirier, G. G.; Droit, A.; Ouellette, M. Quantitative Proteomic Analysis of Amphotericin B Resistance in Leishmania Infantum. *Int. J. Parasitol.: Drugs Drug Resist.* **2014**, *4*, 126−132.
(32) Gao, P.; Liu, Y. Q.; Xiao, W.; Xia, F.; Chen, J. Y.; Gu, L. W.; Yang, F.; Zheng, L. H.; Zhang, J. Z.; Zhang, Q.; Li, Z. J.; Meng, Y. Q.; Zhu, Y. P.; Tang, H.; Shi, Q. L.; Guo, Q. Y.; Zhang, Y.; Xu, C. C.; Dai, L. Y.; Wang, J. G. Identification of Antimalarial Targets of Chloroquine by a Combined Deconvolution Strategy of ABPP and MS-CETSA. *Mil. Med. Res.* **2022**, *9*, 30.
(33) Forte, B.; Ottilie, S.; Plater, A.; Campo, B.; Dechering, K. J.; Gamo, F. J.; Goldberg, D. E.; Istvan, E. S.; Lee, M.; Lukens, A. K.; McNamara, C. W.; Niles, J. C.; Okombo, J.; Pasaje, C. F. A.; Siegel, M. G.; Wirth, D.; Wyllie, S.; Fidock, D. A.; Baragaña, B.; Winzeler, E. A.; Gilbert, I. H. Prioritization of Molecular Targets for Antimalarial Drug Discovery. *ACS Infect. Dis.* **2021**, *7*, 2764−2776.
(34) Birnbaum, J.; Flemming, S.; Reichard, N.; Soares, A. B.; Mesén-Ramírez, P.; Jonscher, E.; Bergmann, B.; Spielmann, T. A Genetic System to Study Plasmodium Falciparum Protein Function. *Nat. Methods* **2017**, *14*, 450−456.
(35) Aurrecoechea, C.; Brestelli, J.; Brunk, B. P.; Dommer, J.; Fischer, S.; Gajria, B.; Gao, X.; Gingle, A.; Grant, G.; Harb, O. S.; Heiges, M.; Innamorato, F.; Iodice, J.; Kissinger, J. C.; Kraemer, E.; Li, W.; Miller, J. A.; Nayak, V.; Pennington, C.; Pinney, D. F.; Roos, D. S.; Ross, C.; Stoeckert, C. J.; Treatman, C.; Wang, H. PlasmoDB: A Functional Genomic Database for Malaria Parasites. *Nucleic Acids Res.* **2009**, *37*, D539.
(36) Trager, W.; Jensen, J. B. Human Malaria Parasites in Continuous Culture. *Science* **1976**, *193*, 673−675.
(37) Moll, K.; Kaneko, A.; Scherf, A.; Wahlgren, M. *Methods in Malaria Research*., 6th edition.; Glasgow, UK, EVIMalaR, 2013.
(38) Wu, Y.; Sifri, C. D.; Lei, H. H.; Su, X. Z.; Wellems, T. E. Transfection of Plasmodium Falciparum within Human Red Blood Cells. *Proc. Natl. Acad. Sci. U. S. A.* **1995**, *92*, 973−977.
(39) Rosario, V. Cloning of Naturally Occurring Mixed Infections of Malaria Parasites. *Science* **1981**, *212*, 1037−1038.
(40) Schneider, C. A.; Rasband, W. S.; Eliceiri, K. W. NIH Image to ImageJ: 25 Years of Image Analysis. *Nat. Methods* **2012**, *9*, 671−675.

https://doi.org/10.1021/acsinfecdis.3c00127
ACS Infect. Dis. 2023, 9, 1257−1266